Journal of Food Engineering 222 (2018) 54–62

Contents lists available at ScienceDirect

Journal of Food Engineering

journal homepage: www.elsevier.com/locate/jfoodeng

Production and characterization of electrospun fish sarcoplasmic protein based nanofibers

Yesim M. Sahin [a, b, *], Sena Su [c, d], Burak Ozbek [c, d], Sevil Yücel [e], Orkun Pinar [f], Dilek Kazan [f], Faik N. Oktar [d, f], Nazmi Ekren [d, g], Oguzhan Gunduz [c, d, **]

[a] Department of Biomedical Engineering, Istanbul Arel University, 34537, Istanbul, Turkey
[b] Polymer Technologies and Composite Materials R & D (ArelPOTKAM), Istanbul Arel University, 34537, Istanbul, Turkey
[c] Department of Metallurgical and Materials Engineering, Faculty of Technology, Marmara University, 34722, Istanbul, Turkey
[d] Advanced Nanomaterials Research Laboratory, Marmara University, 34722, Istanbul, Turkey
[e] Department of Bioengineering, Faculty of Chemical-Metallurgical, Yıldız Technical University, 34220, Istanbul, Turkey
[f] Department of Bioengineering, Faculty of Engineering, Marmara University, 34722, Istanbul, Turkey
[g] Department of Electrical and Electronics Engineering, Faculty of Technology, Marmara University, 34722, Istanbul, Turkey

ARTICLE INFO

Article history:
Received 20 September 2017
Received in revised form
2 November 2017
Accepted 12 November 2017
Available online 15 November 2017

Keywords:
Composite nanofibers
Electrospinning technique
Fish sarcoplasmic protein
Nanomaterials
Polycaprolactone
Tensile strength

ABSTRACT

In this study, poly (ε-caprolactone) (PCL) and fish sarcoplasmic protein (FSP) (Mw < 200 kDa) composite nanofibers were fabricated by electrospinning technique. Solution properties such as density, viscosity, conductivity and surface tension were studied as a function of FSP content in the solution. The morphology, molecular interaction, degradation as well as thermal and tensile properties of PCL/FSP nanofibers were investigated. The results show that smooth and beadless PCL/FSP nanofibers with the diameters ranging from 120 ± 29 nm to 139 ± 41 nm were obtained. The average diameters decreased and the diameter distributions narrowed with the addition of optimum FSP amount. The characteristic picks of FSP and PCL were identified in the composite nanofibers by structural analyses. PCL/FSP nanofibers exhibited high degradation ability in comparison to electrospun pure PCL nanofibers. Moreover, the PCL/FSP nanofibers exhibit good mechanical properties (tensile strength of 5.55 MPa) with the additional FSP content.

1. Introduction

Nanofibers are attractive materials with diameters ranging from 50 to 500 nm having desirable features such as high porosity with very small pore size, high surface area-to-volume ratio, high gas permeability and excellent mechanical properties. Owing to these outstanding properties, these materials are preferred by many researchers and companies in several applications such as delivery systems, tissue engineering, scaffolds, wound healing, biosensors, membrane technology, protective clothing and packaging (Amna et al., 2014; Luo et al., 2010; Okutan et al., 2014; Subbiah et al., 2005).

Electrospinning is one of the versatile and simple techniques for generating continuous ultrathin fibers by using high electrical field to overcome the surface tension of the polymer solution (Agarwal et al., 2008; Ghorani and Tucker, 2015; Zeleny, 1917). Polymer solution properties and processing conditions can be adjusted to optimize nanofiber morphologies and characteristics (Bhardwaj and Kundu, 2010; Reneker and Chun, 1996).

There are many studies on the production of functional nanomaterials from proteins, carbohydrates and lipids (Barnes et al., 2006; Stijnman et al., 2011; Yu et al., 2015). Among these, proteins and peptides have certain advantages such as being biodegradable, nutritive, absorbable and having specific biochemical information (Khadka and Haynie, 2012; Nieuwland et al., 2013). Over the past decade, many researchers have focused on producing and characterizing nanofibers based on plant or animal derived proteins such as soy protein, gelatin and silk fibroin (Cho et al., 2012; Li et al., 2006; Zhang et al., 2005). Most of them have been intended to be used in biomedical industry. Many studies have also shown that some proteins (i.e. egg albumen, soy protein, whey

* Corresponding author. Department of Biomedical Engineering, Istanbul Arel University, 34537, Istanbul, Turkey.
** Corresponding author. Department of Metallurgical and Materials Engineering, Faculty of Technology, Marmara University, 34722, Istanbul, Turkey.
E-mail addresses: ymsahin@arel.edu.tr (Y.M. Sahin), ucemogu@ucl.ac.uk (O. Gunduz).

https://doi.org/10.1016/j.jfoodeng.2017.11.013
0260-8774/

isolate) cannot be spun solitarily and need some carrier systems such as plasticizers and reducing agents (Khadka and Haynie, 2012). Another solution to overcome this difficulty is to blend them with readily spinnable polymers (Colin-Orozco et al., 2014; Pakravan et al., 2011).

Fish sarcoplasmic proteins (FSP) exist in the structure of muscles and are soluble in water or in low ionic strength solution. Sarcoplasmic proteins are included as 20–40% of the total protein content in fish muscle depending on the species (Venugopal and Shahidi, 1996). The Atlantic bonito (*Sarda sarda*, Bloch 1793) is a fish with a wide geographical distribution covering the Atlantic Ocean, the Mediterranean and its bordering seas. Furthermore, it is an abundant and low-cost fish in Turkey.

Moreover, FSP content can be isolated from the wastewater of fish industry. Flesh mince should be repeatedly washed with water in the surimi processing to remove the sarcoplasmic proteins, which lead to a deterioration during storage. On the other hand, these proteins present promising bioactive properties. As an example, these proteins exhibited an inhibitory effect on the dipeptidyl peptidase-4 (DPP-IV) enzyme which is linked to the type-2 diabetes and improve insulin sensitivity in insulin-resistant subjects (Li-Chan et al., 2012; Ouellet et al., 2008). Several recent studies have discussed electrospun fish sarcoplasmic proteins in terms of drug delivery systems and biomaterial applications (Sett et al., 2016; Stephansen et al., 2014).

The present study preferred poly (ε-caprolactone) (PCL) as the polymeric carrier system since it is a commonly used, biodegradable, biocompatible and non-toxic material exhibiting good mechanical properties (Azimi et al., 2014; Kim, 2008). This study aims to produce electrospun nanofibers from fish sarcoplasmic protein and polycaprolactone (PCL) composites and contribute to the relevant research by evaluating their properties as a function of FSP content for the first time in the literature. FSP was obtained from the Atlantic bonito (*sarda sarda*) and its protein composition was investigated. Physical properties of the system such as density, electrical conductivity, viscosity and surface tension were investigated in the study. The degradation behavior as well as the morphological, thermal and mechanical properties of the resultant PCL/FSP nanocomposites were carefully characterized.

2. Materials and methods

2.1. Materials

The Atlantic bonito (*sarda sarda*) from the Black Sea with the length of 35–40 cm was supplied from a local fish market in Küçükyalı, İstanbul. Therefore, fresh fish were eviscerated and filleted manually. All samples were packed and stored at −30°C until they were required. Tetrahydrofuran (THF) and dimethyl formamide (DMF) were supplied by Merck KGaA, Germany. Poly ε-caprolactone (PCL, 80 kDa) was purchased from Sigma-Aldrich, UK.

2.2. Methods

2.2.1. Sarcoplasmic protein (SP) preparation

Frozen fillets were thawed in a refrigerator (4 °C) overnight before used. They were chopped and homogenized with 2.5 vol of de-ionized water in a blender for 1 min. The homogenate was put into tubes and centrifuged at 10,000 × g for 20 min. A part of supernatant (SP solution) was utilized in order to determine its protein patterns with the sodium dodecyl sulfate gel electrophoresis (SDS-PAGE) and the rest of it was freeze dried (Alpha 1–2 LD Plus; Christ, Osterode am Harz, Germany). Preparation of the freeze dried (FD) FSP is illustrated in Fig. 1.

2.2.2. Preparation of spinning solutions

PCL powder was dissolved in a mixed solvent of THF/DMF (7:3, v/v) in a concentration of 6% (w/v). After the complete dissolution of 3% (w/v), 5% (w/v) and 8% (w/v) FSP content in the polymeric liquor by stirring overnight at room temperature, the homogeneous electrospinning solution was obtained. The syringes were connected to the electrospinning system via a plastic syringe with an 18-gauge needle.

2.2.3. Characterization of the polymer solutions

The viscosity of the polymer solution was determined by a digital viscometer (DV-E, Brookfield AMETEK, USA). The density was measured by using a 10 mL specific gravity bottle. The electrical conductivity of the solution was evaluated by a digital conductivity meter (Cond 3110 SET 1,WTW, Germany). A force tensiometer (Sigma 703D, Attension, Germany) was used to measure the surface tension of the polymer solution according to the du Nouy procedure with a platinum ring. All the measurements were performed at room temperature (25 °C).

2.2.4. Fabrication of PCL/FSP nanofibers by electrospinning

Composite nanofibers were prepared by using a laboratory scale electrospinning unit (NS24, Inovenso Co., Turkey). The stainless steel needle (ID: 0.3 mm and OD: 0.8 mm) was connected to a syringe controlled by a syringe pump (NE-300, New Era Pump Systems, Inc., USA), while the pump was used to control the flow rate through the needle. At the beginning of spinning process, the polymer solution was placed into the syringe and then high voltage was applied between the needle and the collector. During the spinning process, circular collector was covered with wax-paper for collecting the nanofibers and the distance of needle tip to the collector was settled as 13 cm. The electrospinning process was performed at the 20 kV applied voltage and 0.4 mL/h flow rate. All the experiments were conducted at room temperature and relative humidity was hold between 40% and 50%.

2.2.5. Protein composition of FSP

Protein composition of FSP extract and freeze dried fish sarcoplasmic protein (FD FSP) were determined by sodium dodecyl sulphate polyacrylamide gel electrophoresis (SDS-PAGE) according to the method of Laemmli (1970) by using 5% (w/v) stacking gel and a 12% (w/v) resolving gel. The protein concentration in the FD FSP extract was estimated 55 mg/mL by Bradford protein assay (Bradford, 1976). FD FSP sample of 27.5 mg was added to an Eppendorf tube together with 0.5 mL demineralized water, dissolved and centrifuged. The supernatant was used to determine protein composition (Stephansen et al., 2014). Electrophoresis was performed at a constant 100 V for 15 min and 120 V for 75 min in Tris-glycine buffer, pH 8.3. The samples were denatured by being boiled for 3 min before they were loaded onto the gel. After the electrophoresis, proteins in the separating gel were visualized by coomassie staining. Fermentas Protein Molecular Weight Marker (Pierce™ Unstained Protein MW Marker, Thermo Fisher Scientific, USA) containing seven proteins within 14.4–116 kDa range was used in order to determine the molecular weight range of the proteins by the Image Analyzer System (Chemi Doc MP Imaging System-BioRad, USA).

2.2.6. Microscopy analysis of the morphologies of the composite nanofibers

The morphologies of composite nanofibers were observed under a scanning electron microscope (SEM) (EVO LS 10, ZEISS) at an accelerating voltage of 10 kV. The average fiber diameter and their distribution were determined by the image analysis software (SmartSEM, Zeiss) using the measurement of 100 fiber selected

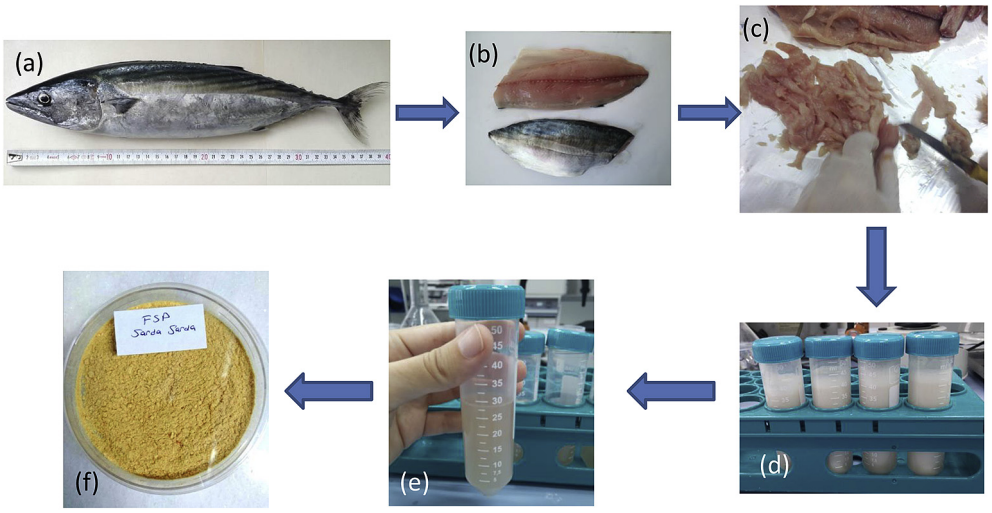

Fig. 1. Preparation steps of freeze-dried fish sarcoplasmic protein powder a) Fresh bonito of 35–40 cm length b) filleted c) chopped d) homogenized with deionized water before the centrifuge e) left supernatant (FSP solution) f) freeze dried FSP powder.

randomly from each sample.

2.2.7. Fourier-transform infrared spectroscopy (FT-IR) of the PCL/FSP composite nanofibers

The FT-IR spectra of the PCL/FSP composite nanofibers were recorded on a Spectrum Two spectrometer (PerkinElmer, Waltham, MA, USA). Each spectrum was collected at the wavenumber range of 400–4000 cm^{-1} and averaged over 128 scans with 4 cm^{-1} resolution. Spectrum™ 10 software from PerkinElmer was used to analyze the spectra.

2.2.8. In vitro degradation study of electrospun PCL/FSP nanocomposites

The in vitro degradation of the electrospun PCL/FSP nanocomposites were evaluated according to the procedure described by Meng et al. (Meng et al., 2010). The selected electrospun nanocomposites were cut into 2 cm × 2 cm pieces, weighted and placed at 37 °C in sealed glass bottles containing 7 mL of phosphate buffer solution (pH 7.4) for up to 8 weeks. After each degradation period (7 days), the samples were washed with deionized water and dried at room temperature for 24 h. Weight loss (%) was calculated using the following equation:

$$\text{Weight loss (\%)} = (Wo - Wt) / Wo \times 100$$

in which W_0 is the weight of each sample before the immersion into the buffer solution, while Wt is the dry weights of the nanocomposite samples after the immersion in the buffer solution for 24 h. Every sample was tested based on three parallels.

2.2.9. Differential scanning calorimetry (DSC)

The thermal properties of the electrospun nanofibers were examined by using a differential scanning calorimeter (Hitachi DSC-7000X, Japan). All samples were analyzed in the temperature range from −30 to 130 °C at a heating rate of 10° C min^{-1} and all measurements were conducted under a nitrogen atmosphere.

2.2.10. Tensile mechanical properties of nanofibers

Mechanical properties of the obtained composites were tested and evaluated with a tensile strength measurement device (INSTRON 4411, Bluehill 2, Elancourt, France) at room temperature (23 °C). Three rectangular shaped (1 × 5cm) testing specimen were prepared for each sample and the thicknesses of the samples were measured by a digital micrometer. Their ends (in the longest direction) are clamped by the top and bottom grips of the device and they are subjected to tensile measurements with 5 mm min^{-1}crosshead speed until the breaking point.

3. Results and discussion

3.1. Physical properties of the polymer solutions

It is now well established from a variety of studies that physical properties of a precursor polymer solution such as density, viscosity, surface tension and conductivity play an important role in the formation of nanofibers during the electrospinning process (Fong et al., 1999; Thompson et al., 2007). The concentration and the viscosity affect the spinnability of the solution, fiber structure and the diameter of the produced nanocomposites. The charged jet fragments into micro/nano particles before reaching to the collector by the effect of the applied voltage and surface tension of the polymeric solution. As the concentration is very low, electrospray occurs instead of electrospinning. However, the solution viscosity becomes exceedingly high at an increased polymeric concentration beyond a critical value and this can hinder the continuous flow of the polymer solution through capillary, which ultimately results in defective or beaded nanofibers (Pillay et al., 2013). High surface tension is generally known to inhibit the electrospinning process. The surface tension must be low enough to obtain continuous nanofibers with well-defined morphologies. Moreover, the electrical field must be at a sufficient strength to overcome the surface tension of the polymer solution (Haghi and Akbari, 2007; Pham et al., 2006). It is well known that electrical conductivity plays a vital role in the structure of the obtained fibers. Data from several studies have shown that the increased electrical conductivity of the polymer solution can eliminate the bead formation and decrease the fiber diameter (Mit-uppatham, Nithitanakul and Supaphol, 2004; Ramakrishna, 2005).

The employed parameters of the PCL/FSP solution at different concentrations are shown in the Fig. 2. The viscosity value was observed that FSP composition was decreased with the interactions and entanglements between molecular chains were weakened. The

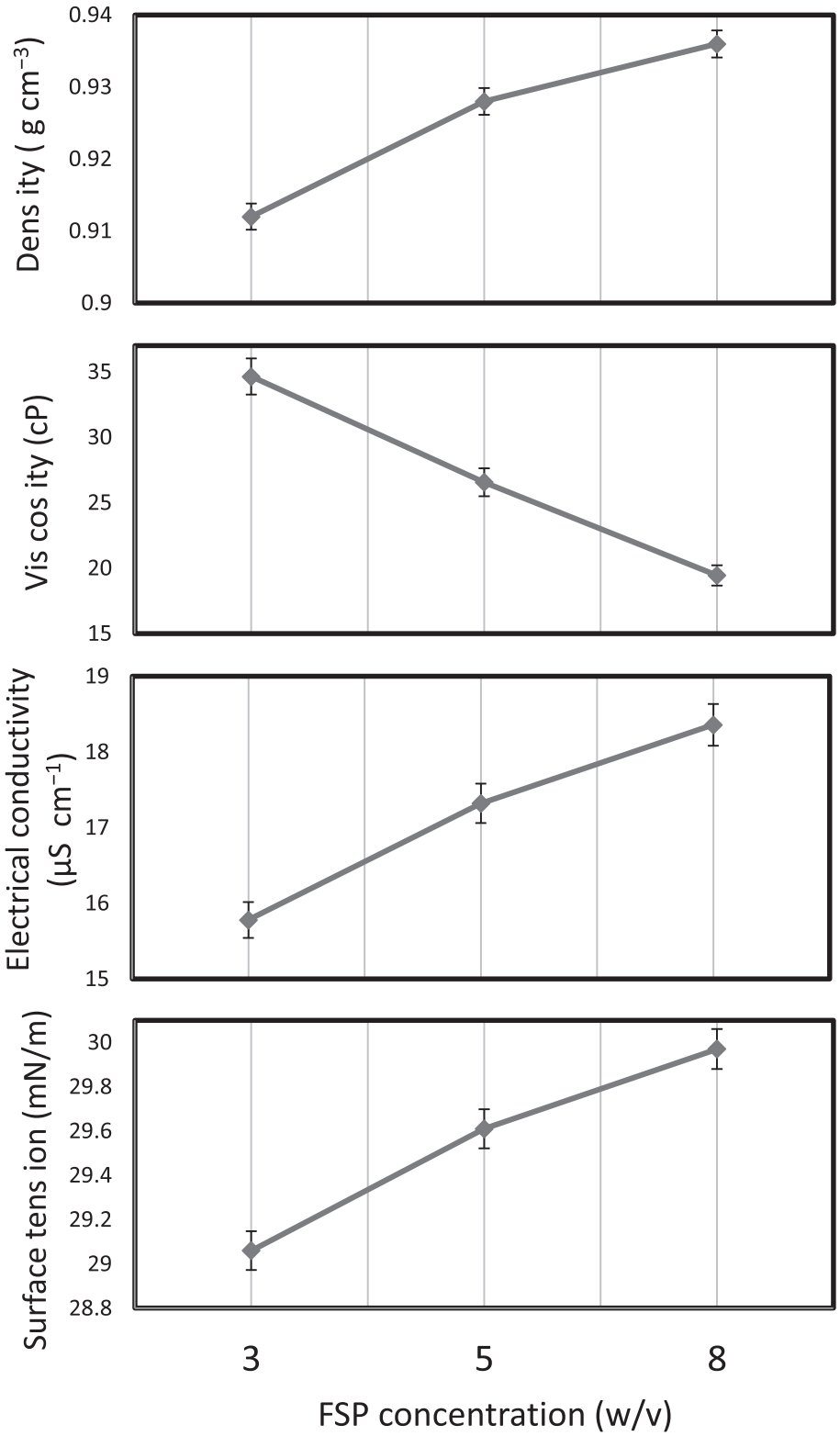

Fig. 2. Density (a), electrical conductivity (b), viscosity (c) and surface tension (d) of blend polymer solution as a function of FSP concentration.

result is also in a good agreement with the previously reported studies (Wongsasulak et al., 2010), which reveal viscosity decrease with an extra globular protein addition. Besides, an increased FSP concentration elevated the electrical conductivity of the solution owing to its polyelectrolyte character.

3.2. Morphological characterization of nanofibers

SEM images of the prepared composite nanofibers having different concentrations of FSP are shown in Fig. 3. All the PCL/FSP composite nanofibers were smooth, beadless and randomly

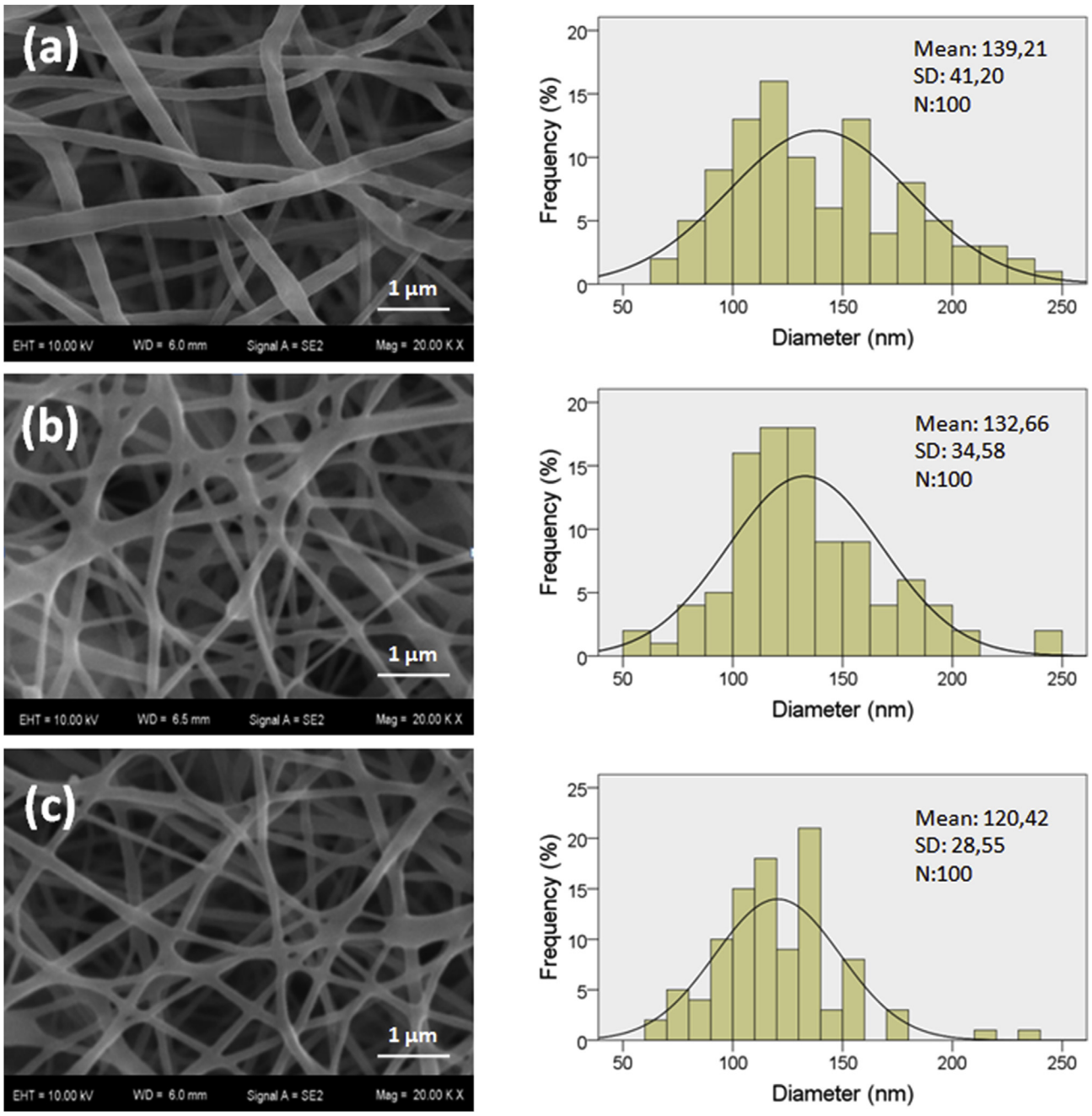

Fig. 3. SEM images and fiber diameter distribution of electrospun PCL/FSP nanofibers with different FSP concentration a) 3% (w/v) b) 5% (w/v) c) 8% (w/v).

oriented. The micrographs indicated that there was no phase separation between the phases during the electrospinning process and the FSP content were observed to be successfully dispersed in the PCL matrix. Average diameters of the PCL/FSP composite nanofibers having 6% (w/v) PCL and 3% (w/v), 5% (w/v), 8% (w/v) FSP were recorded as 139.21 ± 41.20 nm, 131.56 ± 38.47 nm and 120.52 ± 29.48 nm, respectively (Fig. 3a, b and 3c). By increasing the FSP proportion in the PCL/FSP blend solution, the average diameters of the nanofibers were decreased significantly. This result can be attributed to the increased FSP concentration, viscosity decrease and electrical conductivity increase of the system providing thinner nanofibers. Similar findings have also been reported by a study performed with different globular protein (Cho et al., 2012). It should be pointed out that the obtained fiber diameters in this study is thinner than those of the previous studies which were conducted with different proteins and polymers (Cho et al., 2012; He et al., 2017; Wongsasulak et al., 2007). As can be seen in Figs. 3c and 8 % (w/v) FSP had the thinnest fiber average diameter and the lowest standard deviation among all test fibers, however, it presented more curved and irregular shapes than the 3% (w/v) FSP nanofibers. This can be attributed to the higher jet blanching due to the increased electrical conductivity of the solution. As can be seen that no appreciable change was observed in the surface tension by the increment of FSP proportion. Therefore, there was no bead formation resulting from the increased surface tension. On the other hand, the range of diameter distribution narrowed with FSP concentration. It was proved that more homogenous nanofibers can be obtained by adding FSP.

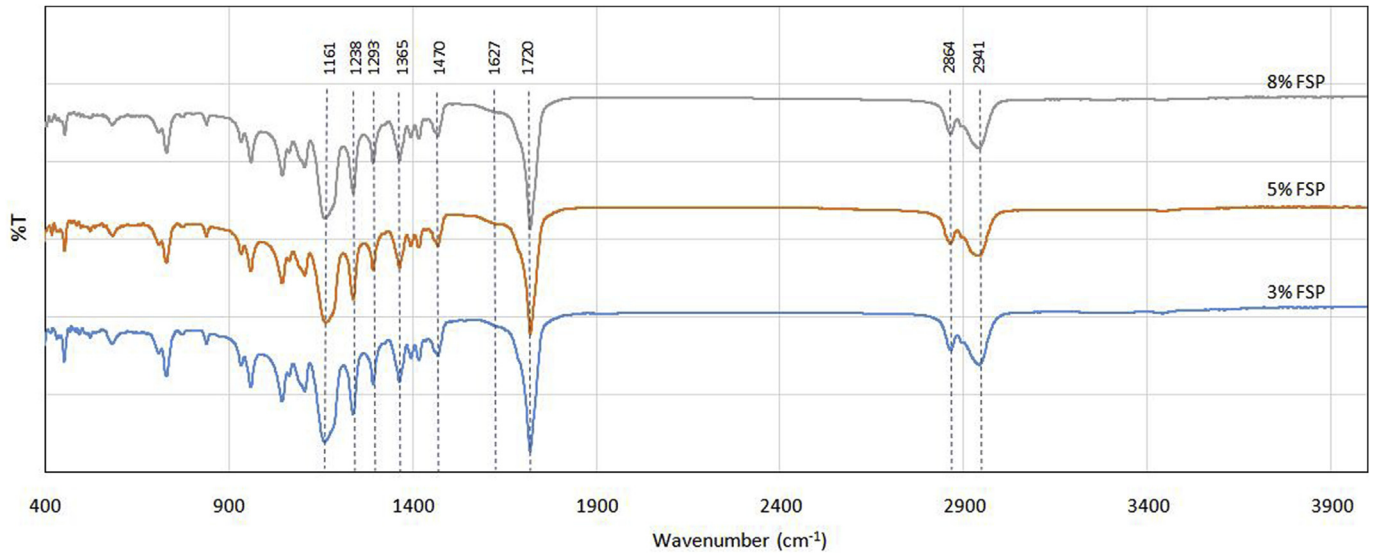

Fig. 4. FT-IR spectrum of PCL/FSP composite nanofibers.

3.3. Fourier-transform infrared spectroscopy (FT-IR)

FT-IR is an effective technique used for identifying the functional groups of complex structures. FTIR spectra of PCL, FD FSP and the produced nanofibers with different concentrations were depicted in Fig. 4. Several characteristic infrared bands of PCL were observed at 2941 cm^{-1} (asymmetric CH2 stretching), 2864 cm^{-1} (symmetric CH2 stretching), 1720 cm^{-1} (carbonyl stretching), 1293 cm^{-1}(C-O and C-C stretching), 1238 cm^{-1} (asymmetric C-O-C stretching) and 1161 cm^{-1} (symmetric C-O-C stretching) (Elzein et al., 2004). It was also observed that PCL/FSP fiber mats showed characteristic protein bands at 1470 and 1365 cm^{-1}corresponding to the N-H bending (amide II) and the combination of the N-H bending and the C-N stretching (amide III), respectively. PCL showed dominant peaks due to the small amount of FSP in the PCL/FSP nanofibers. However, a small peak was also visible at 1627 cm^{-1} attributed to C-O stretching (amide I) belonging to FSP structure (Barth, 2007). All the results imply that PCL/FSP composite nanofibers were

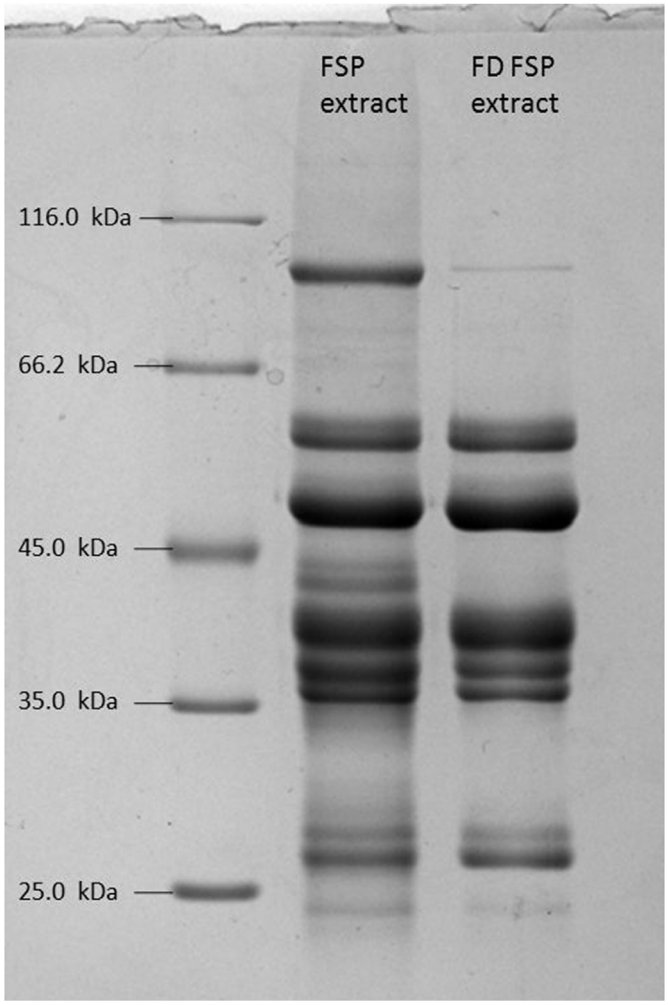

Fig. 5. SDS-PAGE Electrophoresis of FSP extract (lane 1) and FD FSP extract (lane 2).

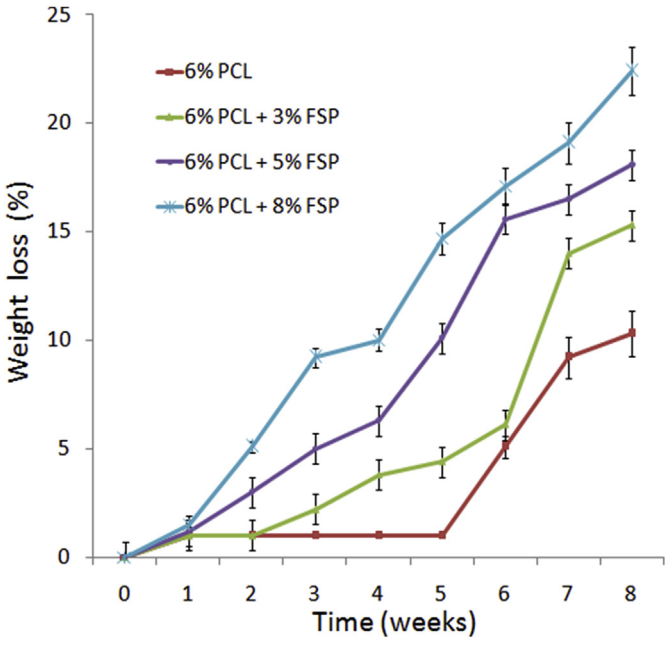

Fig. 6. In vitro degradation of electrospun PCL and PCL/FSP composite nanofibers in PBS (pH 7.4) at 37 °C.

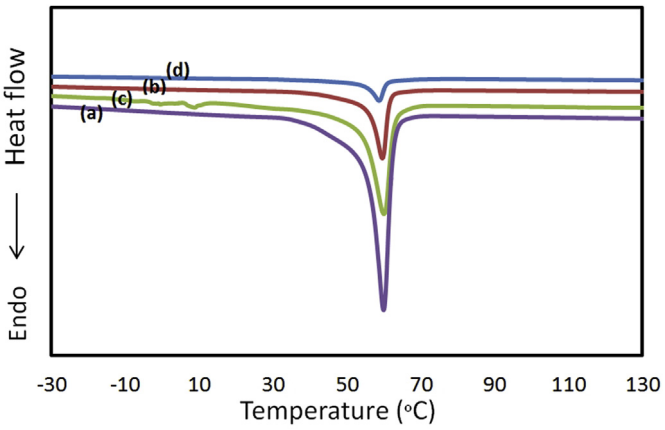

Fig. 7. DSC curves of a) Pure PCL b) 3% (w/v) FSP c) 5% (w/v) FSP d) 8% (w/v) FSP.

successfully produced by the electrospinning process.

3.4. Analysis of FSP protein composition by SDS-PAGE

SDS-PAGE (sodium dodecyl sulphate-polyacrylamide gel electrophoresis) is commonly used for characterization of proteins. Proteins in the sample were separated depending on their molecular weight by this technique. Protein composition of FSP extract (before freeze dried) and FD FSP (after freeze dried) were analyzed by SDS-PAGE to identify its protein patterns and investigate any change of material during processing. As illustrated in Fig. 5, protein band patterns of two samples (FSP extract and FD FSP) are similar. As a result of SDS-PAGE, it is suggested that the protein composition of two samples are very alike. This shows that FD FSP which was used in the preparation of composite nanofiber is successfully produced without an important loss. The protein patterns with the molecular weights (MW) ranging from 23 to 94 kDa were observed and it was identified that the 38,40 and 48 kDa patterns were the most intense ones. These observations are mainly consistent with other studies (Hemung and Chin, 2013; Lopez-Enriquez et al., 2015).

3.5. In vitro degradation

It is commonly known that the long time degradation of PCL limits its use in many applications, especially in the biomedical field. For this reason, the effects of FSP on the biodegradability of PCL have been studied. In vitro degradation behaviors of the electrospun 6% PCL with 3% (w/v), 5% (w/v) and 8% (w/v) FSP were investigated in PBS at 37 °C up to 8 weeks and pure electrospun 6% PCL nanofibers used as control medium. As can be seen from Fig. 6, no change was observed in the weight loss of the pure PCL nanofibers within the first 5-weeks. 5% and 8% FSP nanofibers showed obvious degradation behavior starting from the second week. 3% FSP nanofibers started to lose weight after the third week. As exhibited in Fig. 6, the percentage of the weight loss of 3%, 5% and 8% FSP nanofibers was 15.3%, 18.1% and 22.4% after 8 week

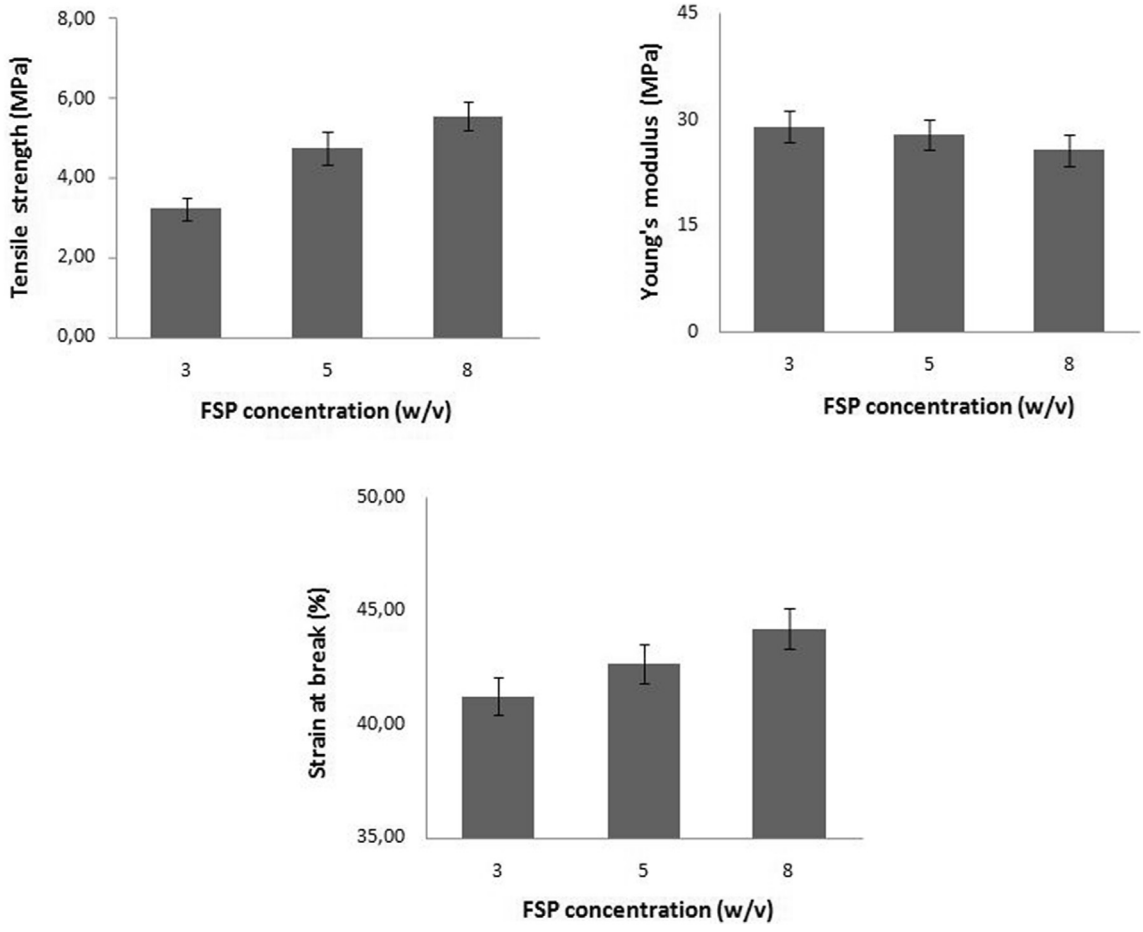

Fig. 8. Tensile properties of composite nanofibers versus FSP concentration a) Tensile strength, b) Young's modulus and c) Strain at break.

Table 1
Melting temperatures and enthalpy values of nanofibers.

Samples	Tm (°C)	ΔHm (j/g)
Pure PCL	60.1	135
3% (w/v) FSP	59.5	104
5% (w/v) FSP	59.1	64.5
8% (w/v) FSP	58.5	49.1

immersions, respectively. Pure PCL nanofibers have a weight loss of 10.3% over the degradation period. It can be clearly seen that the degradation rates of PCL/FSP composite nanofibers were much faster than for pure PCL nanofibers. This result may be explained by the fact that amide groups in the FSP are able to form hydrogen bonds with water molecules, which give FSP its hydrophilic structure. Therefore, addition of FSP increased the hydrophilicity of PCL nanofibers.

3.6. Thermal properties

Thermal properties of pure PCL and PCL/FSP nanofibers were measured by DSC and their DSC curves, melting peak temperatures and enthalpy values of the nanofibers are presented in Fig. 7 and Table 1. Nanocomposites exhibited sharp endothermic curves at about 59 °C since the polymer chains fell out of their crystal structures and indicated a melting curve. The melting point slightly decreased with the additional FSP content as shown in Table 1. It was also observed that the melting enthalpy of the nanofibers decreased from 135 J g^{-1}(Pure PCL) to 49.1 J g^{-1} (8% FSP) by the incorporation of FSP content. This result showed that FSP has a reducing effect on the crystallinity of PCL nanofibers. He et al. (2017) reported that they found similar results with incorporation of the protein (keratin) decreased the melting enthalpy of the poly (vinyl alcohol) nanofibers.

3.7. Tensile properties

Tensile measurement for each PCL/FSP composite nanofiber having different FSP proportions is shown in Fig. 8. It can be seen from Fig. 8 that an increase in the FSP concentration led to a considerable increase in the tensile strength of composite nanofiber mats. Optimum FSP concentration value was identified as 8% (w/v) due to the highest tensile strength of the 5.55 MPa. This observation can be explained by a decrease in the fiber diameter and fiber distribution range with FSP content, as shown in Fig. 2. Nanofibrous material with smaller fiber diameter and distribution demonstrated better mechanical properties due to high surface area to volume ratio and a cohesion increment between the nanofibers was observed. Similar effects were reported by the previously published studies (Wong et al., 2008; Meng et al., 2010). The values of young modulus (E) and strain at break (%) for different concentrations of the PCL/FSP nanofiber mat are represented in Fig. 8b and c. The mean value of Young's modulus for all the samples were in the range of 24.7–29.1 MPa and decreased with FSP proportion. Furthermore, the values of strain at break showed a gradual increase from 41.2% to 44.1% with the increasing FSP ratio. These results are consistent with the previous reports on the tensile properties of composite nanofibers obtained from different proteins and polymers (Khadka and Haynie, 2012; Zhang et al., 2005). On the other hand, this finding is contrary to a relevant study which reported that the mechanical strength of electrospun nanofiber mats decreased as the protein content increased (Cho et al., 2012). It may be attributed to that tensile characteristic behaviors are mostly based on the material properties and the strength of interactions between polymers.

To sum up, these results indicate that the FSP content is an important factor for tensile properties of PCL/FSP composite systems. This makes FSP a promising material, which can be used in various applications including wound dressing and biodegradable packaging, in which tensile strength, is one of the most desirable characteristics.

4. Conclusion

In this study, PCL/FSP nanofibers were successfully fabricated by the electrospinning technique. Fish sarcoplasmic protein (FSP) was extracted from the Atlantic bonito, lyophilized and their protein composition was revealed by SDS-PAGE. FSP was incorporated to polymeric matrix, PCL, at different concentrations. The conductivity increased and the viscosity decreased depending on the FSP content. According to results obtained in this work, addition of FSP changed the morphology and the distribution of nanofibers positively. It is observed that 8% (w/v) PCL/FSP nanofibers exhibited the lowest fiber average diameter (120.52 nm) among all. According to the results of the in vitro degradation analysis, additional FSP content enhanced the biodegradability of the PCL matrix. DSC results indicated that the crystallinity of the PCL nanofibers was reduced with the FSP incorporation. Moreover, the results of tensile test showed that PCL/FSP nanofibers exhibited strong mechanical properties with an increment of FSP content. This could be an interesting material for future studies on the encapsulation and controlled release of food ingredients. To sum up, the present study demonstrates that the FSP based nanocomposites have potential to be used for different applications such as biodegradable packaging, food applications, drug delivery and wound dressing etc. with their enhanced mechanical properties and biodegradability.

Acknowledgements

This work is founded from Marmara University, BAPKO project number: FEN-C-YLP-120417-0177.

References

Agarwal, S., Wendorff, J.H., Greiner, A., 2008. Use of electrospinning technique for biomedical applications. Polymer 49 (26), 5603–5621. https://doi.org/10.1016/j.polymer.2008.09.014.

Amna, T., Yang, J., Ryu, K.S., Hwang, I.H., 2014. Electrospun antimicrobial hybrid mats: innovative packaging material for meat and meat-products. J. Food Sci. Technol. 52 (7), 4600–4606. https://doi.org/10.1007/s13197-014-1508-2.

Azimi, B., Nourpanah, P., Rabiee, M., Arbab, S., 2014. Poly (ε -caprolactone) Fiber: an overview. J. Eng. Fibers Fabr. 9 (3), 74–90.

Barnes, C., Smith, M., Bowlin, G., Sell, S., 2006. Feasibility of electrospinning the globular proteins hemoglobin and myoglobin. J. Eng. Fibers Fabr. 1 (2), 16–29. Retrieved from. http://www.jeffjournal.org/papers/06Dec_Electrospinning.pdf.

Barth, A., 2007. Infrared spectroscopy of proteins. Biochim. Biophys. Acta-Bioenerg. 1767 (9), 1073–1101. https://doi.org/10.1016/j.bbabio.2007.06.004.

Bhardwaj, N., Kundu, S.C., 2010. Electrospinning: a fascinating fiber fabrication technique. Biotechnol. Adv. 28 (3), 325–347. https://doi.org/10.1016/j.biotechadv.2010.01.004.

Cho, D., Netravali, A.N., Joo, Y.L., 2012. Mechanical properties and biodegradability of electrospun soy protein Isolate/PVA hybrid nanofibers. Polym. Degrad. Stab. 97 (5), 747–754. https://doi.org/10.1016/j.polymdegradstab.2012.02.007.

Colin-Orozco, J., Zapata-Torres, M., Rodruguez-Gattorno, G., Pedroza-Islas, R., 2014. Properties of poly (ethylene oxide)/whey protein isolate nanofibers prepared by electrospinning. Food Biophys. 10 (2), 134–144. https://doi.org/10.1007/s11483-014-9372-1.

Elzein, T., Nasser-Eddine, M., Delaite, C., Bistac, S., Dumas, P., 2004. FTIR study of polycaprolactone chain organization at interfaces. J. Colloid Interface Sci. 273 (2), 381–387. https://doi.org/10.1016/j.jcis.2004.02.001.

Fong, H., Chun, I., Reneker, D.H., 1999. Beaded nanofibers formed during electrospinning. Polymer 40, 4585–4592. https://doi.org/10.1016/S0032-3861(99)00068-3.

Ghorani, B., Tucker, N., 2015. Fundamentals of electrospinning as a novel delivery vehicle for bioactive compounds in food nanotechnology. Food Hydrocoll. 51, 227–240. https://doi.org/10.1016/j.foodhyd.2015.05.024.

Haghi, A.K., Akbari, M., 2007. Trends in electrospinning of natural nanofibers. Phys. Status Solidi (A) Appl. Mater. Sci. 204, 1830–1834. https://doi.org/10.1002/pssa.

200675301.
He, M., Zhang, B., Dou, Y., Yin, G., Cui, Y., Chen, X., 2017. Fabrication and characterization of electrospun feather keratin/poly(vinyl alcohol) composite nanofibers. RSC Adv. 7, 9854–9861. https://doi.org/10.1039/c6ra25009b.
Hemung, B.O., Chin, K.B., 2013. Effects of fish sarcoplasmic proteins on the properties of myofibrillar protein gels mediated by microbial transglutaminase. LWT - Food Sci. Technol. 53 (1), 184–190. https://doi.org/10.1016/j.lwt.2013.02.008.
Khadka, D.B., Haynie, D.T., 2012. Protein- and peptide-based electrospun nanofibers in medical biomaterials. Nanomed. Nanotechnol. Biol. Med. 8 (8), 1242–1262. https://doi.org/10.1016/j.nano.2012.02.013.
Kim, G.H., 2008. Electrospun PCL nanofibers with anisotropic mechanical properties as a biomedical scaffold. Biomed. Mater. (Bristol Engl.) 3 (2), 25010. https://doi.org/10.1088/1748-6041/3/2/025010.
Li-Chan, E.C.Y., Hunag, S.L., Jao, C.L., Ho, K.P., Hsu, K.C., 2012. Peptides derived from Atlantic salmon skin gelatin as dipeptidyl-peptidase IV inhibitors. J. Agric. Food Chem. 60 (4), 973–978. https://doi.org/10.1021/jf204720q.
Li, C., Vepari, C., Jin, H.-J., Kim, H.J., Kaplan, D.L., 2006. Electrospun silk-BMP-2 scaffolds for bone tissue engineering. Biomaterials 27 (16), 3115–3124. https://doi.org/10.1016/j.biomaterials.2006.01.022.
Lopez-Enriquez, R.L., Ocano-Higuera, V.M., Torres-Arreola, W., Ezquerra-Brauer, J.M., Marquez-Rios, E., 2015. Chemical and functional characterization of sarcoplasmic proteins from giant squid (Dosidicus gigas) mantle. J. Chem. 2015. https://doi.org/10.1155/2015/538721.
Luo, C.J., Nangrejo, M., Edirisinghe, M., 2010. A novel method of selecting solvents for polymer electrospinning. Polymer 51 (7), 1654–1662. https://doi.org/10.1016/j.polymer.2010.01.031.
Meng, Z.X., Zheng, W., Li, L., Zheng, Y.F., 2010. Fabrication and characterization of three-dimensional nanofiber membrane of PCL-MWCNTs by electrospinning. Mater. Sci. Eng. C 30 (7), 1014–1021. https://doi.org/10.1016/j.msec.2010.05.003.
Mit-Uppatham, C., Nithitanakul, M., Supaphol, P., 2004. Ultratine electrospun polyamide-6 fibers: effect of solution conditions on morphology and average fiber diameter RID C-4353-2008. Macromol. Chem. Phys. 205 (17), 2327–2338. https://doi.org/10.1002/macp.200400225.
Nieuwland, M., Geerdink, P., Brier, P., van den Eijnden, P., Henket, J.T.M.M., Langelaan, M.L.P., et al., 2013. Food-grade electrospinning of proteins. Innovative Food Sci. Emerg. Technol. 20, 269–275. https://doi.org/10.1016/j.ifset.2013.09.004.
Okutan, N., Terzi, P., Altay, F., 2014. Affecting parameters on electrospinning process and characterization of electrospun gelatin nanofibers. Food Hydrocoll. 39, 19–26. https://doi.org/10.1016/j.foodhyd.2013.12.022.
Ouellet, V., Weisnagel, S.J., Marois, J., Bergeron, J., Julien, P., Gougeon, R., et al., 2008. Dietary cod protein reduces plasma C-reactive protein in insulin-resistant men and women. J. Nutr. 138 (12), 2386–2391. https://doi.org/10.3945/jn.108.092346.
Pakravan, M., Heuzey, M.C., Ajji, A., 2011. A fundamental study of chitosan/PEO electrospinning. Polymer 52 (21), 4813–4824. https://doi.org/10.1016/j.polymer.2011.08.034.
Pham, Q.P., Sharma, U., Mikos, A.G., 2006. Electrospun poly (??-caprolactone) microfiber and multilayer nanofiber/microfiber scaffolds: characterization of scaffolds and measurement of cellular infiltration. Biomacromolecules 7 (10), 2796–2805. https://doi.org/10.1021/bm060680j.
Pillay, V., Dott, C., Choonara, Y.E., Tyagi, C., Tomar, L., Kumar, P., et al., 2013. A Review of the Effect of Processing Variables on the Fabrication of Electrospun Nanofibers for Drug Delivery Applications, vol. 2013, p. 22. https://doi.org/10.1155/2013/789289.
Ramakrishna, S.F.K.T.W.L.T.M.Z., 2005. An Introduction to Electrospinning and Nanofibers (Google EBook). Introduction to Electrospinning and Nanofibers. https://doi.org/10.1142/5894.
Reneker, D.H., Chun, I., 1996. Nanometre diameter fibres of polymer, produced by electrospinning. Nanotechnology 7 (3), 216–223. https://doi.org/10.1088/0957-4484/7/3/009.
Sett, S., Stephansen, K., Yarin, A.L., 2016. Solution-blown nanofiber mats from fish sarcoplasmic protein. Polym. (United Kingdom) 93, 78–87. https://doi.org/10.1016/j.polymer.2016.04.019.
Stephansen, K., Chronakis, I.S., Jessen, F., 2014. Bioactive electrospun fish sarcoplasmic proteins as a drug delivery system. Colloids Surfaces B Biointerfaces 122, 158–165. https://doi.org/10.1016/j.colsurfb.2014.06.053.
Stijnman, A.C., Bodnar, I., Hans Tromp, R., 2011. Electrospinning of food-grade polysaccharides. Food Hydrocoll. 25 (5), 1393–1398. https://doi.org/10.1016/j.foodhyd.2011.01.005.
Subbiah, T., Bhat, G.S., Tock, R.W., Parameswaran, S., Ramkumar, S.S., 2005. Electrospinning of nanofibers. J. Appl. Polym. Sci. 96 (2), 557–569. https://doi.org/10.1002/app.21481.
Thompson, C.J., Chase, G.G., Yarin, A.L., Reneker, D.H., 2007. Effects of parameters on nanofiber diameter determined from electrospinning model. Polymer 48 (23), 6913–6922. https://doi.org/10.1016/j.polymer.2007.09.017.
Venugopal, V., Shahidi, F., 1996. Structure and composition of fish muscle. Food Rev. Int. 12 (2), 175–197. https://doi.org/10.1080/87559129609541074.
Wong, S.C., Baji, A., Leng, S., 2008. Effect of fiber diameter on tensile properties of electrospun poly(ε-caprolactone). Polymer 49 (21), 4713–4722. https://doi.org/10.1016/j.polymer.2008.08.022.
Wongsasulak, S., Kit, K.M., McClements, D.J., Yoovidhya, T., Weiss, J., 2007. The effect of solution properties on the morphology of ultrafine electrospun egg albumen-PEO composite fibers. Polymer 48 (2), 448–457. https://doi.org/10.1016/j.polymer.2006.11.025.
Wongsasulak, S., Patapeejumruswong, M., Weiss, J., Supaphol, P., Yoovidhya, T., 2010. Electrospinning of food-grade nanofibers from cellulose acetate and egg albumen blends. J. Food Eng. https://doi.org/10.1016/j.jfoodeng.2010.01.014.
Yu, D.-G., White, K., Chatterton, N., Li, Y., Li, L., Wang, X., 2015. Structural lipid nanoparticles self-assembled from electrospun core–shell polymeric nanocomposites. RSC Adv. https://doi.org/10.1039/C4RA14001J.
Zeleny, J., 1917. Instability of electrified liquid surfaces. Phys. Rev. 10 (1), 1–6. https://doi.org/10.1103/PhysRev.10.1.
Zhang, Y., Ouyang, H., Chwee, T.L., Ramakrishna, S., Huang, Z.M., 2005. Electrospinning of gelatin fibers and gelatin/PCL composite fibrous scaffolds. J. Biomed. Mater. Res. Part B Appl. Biomaterials 72 (1), 156–165. https://doi.org/10.1002/jbm.b.30128.